Cancer Letters 444 (2019) 147–161

Contents lists available at ScienceDirect

Cancer Letters

journal homepage: www.elsevier.com/locate/canlet

Original Articles

Modulation of lung cancer cell plasticity and heterogeneity with the restoration of cisplatin sensitivity by neurotensin antibody

Zherui Wu[a], Ludovic Fournel[a,b,c,1], Nicolas Stadler[a,1], Jin Liu[a,1], Agnès Boullier[d], Nadia Hoyeau[e], Jean François Fléjou[e], Véronique Duchatelle[f], Nouzha Djebrani-Oussedik[g], Mikaël Agopiantz[h], Evelyne Ségal-Bendirdjian[a], Anne Gompel[a,i], Marco Alifano[a,b], Olle Melander[j], Jean Trédaniel[a,k,*], Patricia Forgez[a,**]

[a] INSERM UMRS 1007, Paris Descartes University, 75270, Paris Cedex 06, France
[b] Department of Thoracic Surgery, Cochin Hospital of Paris, AP-HP, Paris Descartes University, Paris, France
[c] Paris-Sud, Paris-Saclay University, Orsay, France
[d] CBH Biochemistry Laboratory, CHU Amiens-Picardie, Amiens, France
[e] Department of Pathology, Saint-Antoine Hospital, AP-HP, UPMC, Paris, France
[f] Department of Pathology, Groupe Hospitalier Paris Saint Joseph, Paris Descartes University, Paris, France
[g] Toxicology Laboratory, Lariboisière Hospital, AP-HP, Paris, France
[h] Department of Pathology, CHRU Nancy, University of Lorraine, Nancy, France
[i] Department of Gynecology Obstetrics II and Reproductive Medicine, Paris Descartes University, AP-HP, Paris, France
[j] Department of Clinical Sciences, Lund University, Skåne University Hospital, CRC, Malmö, Sweden
[k] Unit of Thoracic Oncology, Groupe Hospitalier Paris Saint Joseph, Paris Descartes University, Paris, France

ARTICLE INFO

Keywords:
Anti-tumor drug
Neurotensin antibody
Tumor cell plasticity
Advanced lung cancer
Restoration of platinum salt-based chemotherapy sensitivity

ABSTRACT

Overall survival of patients with metastatic non-small cell lung cancer (NSCLC) has significantly improved with platinum-based salt treatments and recently with targeted therapies and immunotherapies. However, treatment failure occurs due to acquired or emerging tumor resistance.

We developed a monoclonal antibody against the proform of neurotensin (LF-NTS mAb) that alters the homeostasis of tumors overexpressing NTSR1. Neurotensin is frequently overexpressed along with its high affinity receptor (NTSR1) in tumors from epithelial origins. This ligand/receptor complex contributes to the progression of many tumor types by activation of the cellular effects involved in tumor progression (proliferation, survival, migration, and invasion).

We demonstrate that LF-NTS mAb operates on the plasticity of tumor cells overexpressing NTSR1 and lowers their aggressiveness. The mAb enables the restoration of platinum-based therapies responsiveness, while also decreasing metastatic processes. Efficacy dosage with long-term treatment showed no obvious adverse events, while demonstrating improvement in the performance status. Our data suggests that LF-NTS mAb is an ideal candidate to be safely added to the conventional standard of care in order to improve its efficacy.

1. Introduction

Recent advances in treatment of advanced or metastatic non-small cell lung cancer (NSCLC) have significantly improved the overall survival (OS) and the progression-free survival (PFS) of affected patients. Despite substantial improvements in NSCLC treatment, this cancer remains the leading cause of cancer-related death in the world [1].

Lung cancer is a very heterogeneous disease, with non-small cell lung cancer (NSCLC) representing nearly 85% of lung tumors. It is mostly an asymptomatic disease diagnosed at the metastatic stage in at least 60% of cases [2].

Current standard chemotherapy regimens combine platinum-salt compound with an antimetabolite (mostly pemetrexed for adenocarcinoma), or a spindle poison (paclitaxel). This treatment increases the OS up to 12 months or more as compared to 4.5 months with best supportive care [3,4]. Unfortunately, patients still develop incurable and

* Corresponding author. INSERM UMR-S 1007, Université Paris Descartes, 45 rue des Saints-Pères, 75270, Paris cedex 06, France.
** Corresponding author.
E-mail addresses: jtredaniel@hpsj.fr (J. Trédaniel), patricia.forgez@inserm.fr (P. Forgez).
[1] Contribute equally to the work.

https://doi.org/10.1016/j.canlet.2018.12.007
Received 4 October 2018; Received in revised form 5 December 2018; Accepted 11 December 2018

List of abbreviations

AKT	Protein kinase B
ALK	Anaplastic lymphoma kinase
CHO	Chinese hamster ovary
Bcl-2	B-cell Lymphoma 2
DFS	Disease-free survival
EGF	Epidermal growth factor
EGFR	Epidermal growth factor receptor
ELISA	Enzyme-linked immunosorbent assay
ERK	Extracellular signal–regulated kinase
FBS	Fetal bovine serum
GPCR	G protein-coupled receptor
GS-X	Glutathione S-conjugate pumps
HDL	High-density lipoprotein
HER	Human epidermal growth factor
IgG	Immunoglobulin G
LF-NTS	Long-fragment neurotensin
mAb	monoclonal antibody
MRP	Multidrug Resistance-Associated Protein
NSCLC	non small cell lung cancer
NTS	Neurotensin
NTSR1	Neurotensin receptor 1
OS	overall survival
PDX	Patient derived xenografts
RECIST	Response evaluation criteria in solid tumors
RIPK	Receptor-interacting serine/threonine-protein kinase
SOC	Standard of care
TKI	Tyrosine kinase inhibitor
TUNEL	Terminal deoxynucleotidyl transferase dUTP nick end labeling

progressively fatal disease.

Recently, the heterogeneous nature of tumors has been revealed by advanced molecular diagnostics, depicting the genetic constitution of intra-tumor clones. It has become clear that tumor heterogeneity is accountable for the variable range of patient responses [5], while additional experiments revealed that tumor heterogeneity is dynamic in space and time. Spatial heterogeneity, observed within the primary tumor, was also detected between distant sites, organs or lymph nodes, as proven with genetic analysis [6]. Tumor evolution with time was also revealed by genetic changes during the course of the disease, with emergence of new mutations or restoration of the wild type phenotype was observed [5].

The development of biomarkers, identifying driver mutations enabled the deployment of targeted therapies for NSCLC. Targeted therapies are now proposed to the 15–20% of NSCLC patients bearing specific genomic mutations or rearrangements (mainly EGFR and ALK, but also Ros-1 and B-RAF) [7–9]. These less toxic treatments significantly improve OS and quality of life. Nevertheless, the majority of patients ultimately develop resistance. Tumor heterogeneity was responsible for these treatment failures. Indeed, it was shown that resistance to T790M-targeting EGFR-TKI was related to the emergence of wild type clones [10]. In the same vein, immunotherapy (anti-PD-1/PD-L1) was successfully developed [11] and is now proposed as monotherapy to the fraction of patients whose malignant cells are at least 50% positive for PD-L1, representing approximately 30% of the patients. These therapies show satisfactory survival results, with a relatively safe therapeutic profile as compared to conventional chemotherapy [12]. However, only 20–30% of patients are responders, and the duration of response is globally limited and often associated with a panel of immune-related adverse events [13].

Tumor plasticity also becomes a major issue, because resistance can emerge from activation of bypass signaling pathways, cell-lineage changes, or acquired mutations [14–16]. Indeed, tumor physiological characteristics are dynamic, depending on their microenvironment, their access to growth factors by vascularization, the immune environment, and their adaptation to treatment. Several studies have shown that this dynamic aspect of tumors drives them along the progression to a more aggressive, and uncontrollable state, and ultimately promoting drug resistance [17–19]. The dynamic features of tumor cells inferred by their plasticity, makes the development of successful therapy problematic. These adaptive features are not unidirectional and can be modulated, with cells exhibiting a more or less aggressive behavior, independently of the level of its mutational state. The manipulation of tumor cell plasticity to maintain a less aggressive behavior creates a pertinent therapeutic approach to improve the performance of the anti-tumor drugs.

In this context, we show that the decrease of neurotensin receptor 1 activity impacts tumor cell aggressiveness while improving the response to chemotherapy by restoring platinum salt sensitivity. Neurotensin is synthesized from a proform of 170 amino acids, cleaved by convertases to produce NTS and neuromedin N. Missed cleavage of the NTS proform produces Long-Fragment NTS (LF-NTS) which was shown to exhibit the same biological activity as the mature peptide but with greater stability [20]. Circulating LF-NTS is active and is significantly correlated to the development of breast cancer, diabetes, cardiovascular disease, and total mortality [21]. Based on previous results, we hypothesized that following abnormal production of NTS, the immature proform will preferentially be released at the vicinity of the tumor cells, and would induce sustained and intense NTSR1 activation with associated signalization. Indeed, chronic activation with high doses of NTS agonist, in cell lines over expressing NTSR1, induced NTSR1 gene activation and a permanent NTSR1 recycling at the cell surface [22–24]. NTSR1 overstimulation, generated by a permanent NTS autocrine loop, as its occurs in tumors, induces a cascade of cellular events resulting in the activation of metalloproteinases and the release of “EGF like” ligands (Hb-EGF and neuregulins), creating autocrine activating control loops for three major epidermal growth factor receptors (EGFR, HER2, HER3) [25–27]. In an attempt to impair or inhibit these cascading effects, we developed a neutralizing antibody for LF-NTS to inhibit the effect of these cascades. In this paper, we first correlate NTSR1 expression with the response to the combination of platinum and pemetrexed treatment in patients with primitive metastatic lung adenocarcinomas. We demonstrate that LF-NTS mAb acts on the tumor cell plasticity of lung cancer cells. This treatment resulted in the alteration of their aggressiveness by decreasing growth, and the reduction of metastatic processes. By affecting the cellular plasticity, the response to cisplatin treatment was restored while improving physical activity and increasing body weight.

2. Materials and methods

2.1. Patients and tissue specimens for NTS and NTSR1 immunohistochemistry

The clinical files of 28 patients with metastatic stage non-squamous NSCLC, treated with a platinum-pemetrexed doublet regimen, were retrospectively reviewed. Most patients from this series, including 17 (60.7%) men and 11 (39.3%) women, exhibited conventional risk factors for NSCLC, such as smoking (82.1%), chronic obstructive pulmonary disease (15.0%) or professional exposure (6.1%). Pretreatment tumor biopsies established the diagnosis of lung adenocarcinomas in the majority of patients (86.7%) followed by large cell (10.0%) and sarcomatoid (3.3%) carcinomas. Histological slides of lung biopsies were obtained from paraffin wax embedded tissues. Standard

hematoxylin and eosin staining was used to confirm the cancerous character of the specimens, and adjacent sections were obtained for immunohistochemistry. Information concerning Public database are described in supplementary methods.

2.2. Ethics

Informed consent was obtained from all patients before biopsy. The database including pathological variables was established in accordance with the French data protection authority (Ile de France II # 2016-10-05).

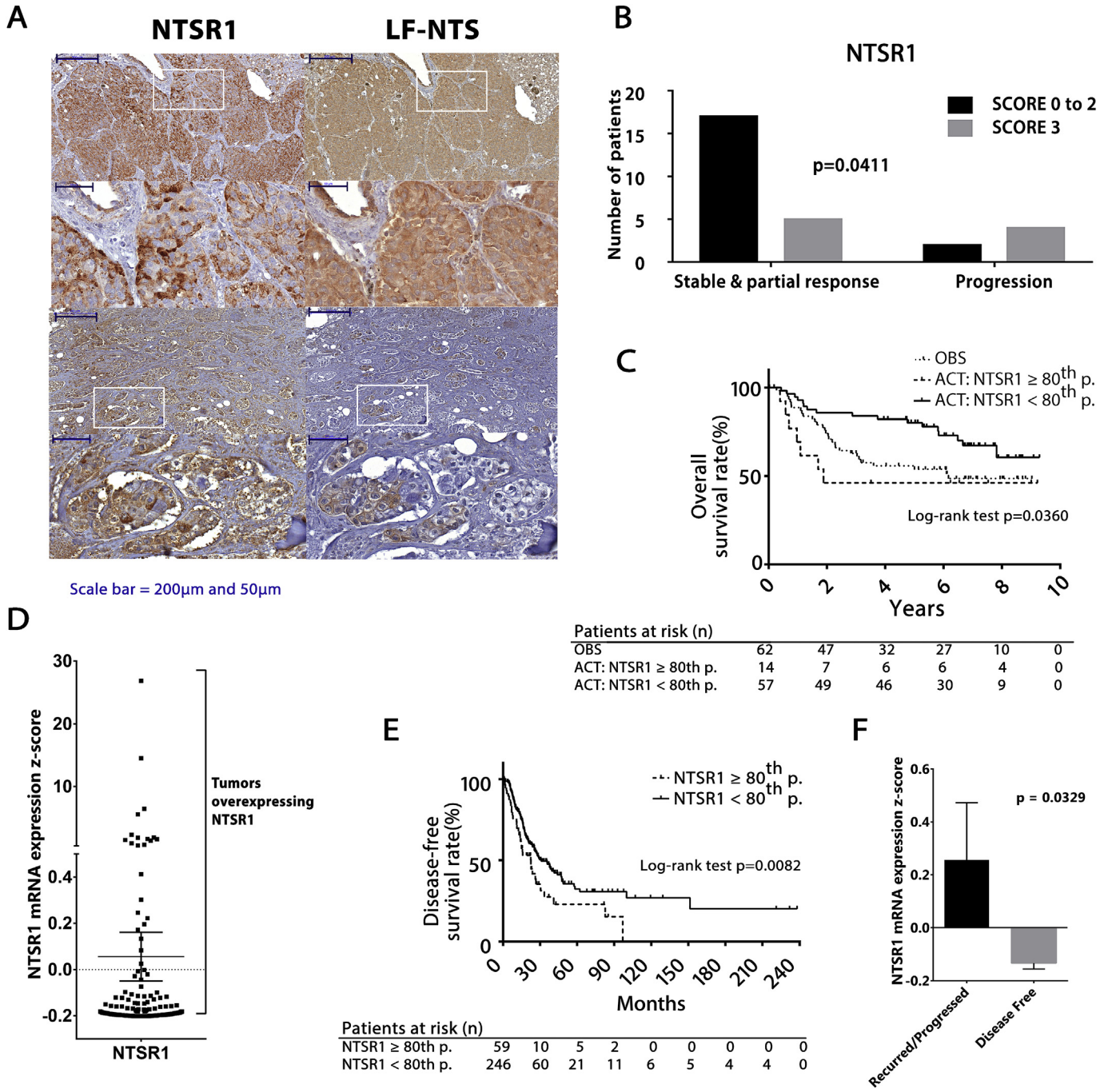

Fig. 1. NTSR1 expression in NSCLC and clinical outcome. **(A)** Immunohistochemistry of NTSR1 and LF-NTS in metastatic stages of non-squamous NSCLC patient biopsies. Examples of positive staining at X100 and X400 magnification. **(B)** Distribution of stable population or with a partial response vs in progression after platinum salt based therapy, according to NTSR1 expression (score from 0 to 2 *vs* score 3) (Pearson chi-square). **(C)** The Kaplan–Meier analysis of overall survival (OS) calculated from patients with NSCLC from stage IB to IIIA (GSE14814, n = 133). (ACT) 71 patients treated with vinorelbine/cisplatin following surgery, (OBS) 62 patients treated by surgery alone. In the ACT group, the OS is analyzed based on the NTSR1 mRNA expression. Patients at risk are noted below the graphs. **(D)** NTSR1 mRNA distribution (Z-score) of 305 tumor samples from stage IB to IV of lung adenocarcinoma (TCGA-LUAD). **(E)** The Kaplan–Meier analysis of disease-free survival (DFS) based on the NTSR1 mRNA expression in patients from stage IB to IV with lung adenocarcinoma (TCGA-LUAD, n = 305) who received surgery and chemotherapy as initial treatment. Patients at risk are noted below the graphs. **(F)** Distribution of NTSR1 mRNA expression (Z-scores) according to the response to initial treatment.

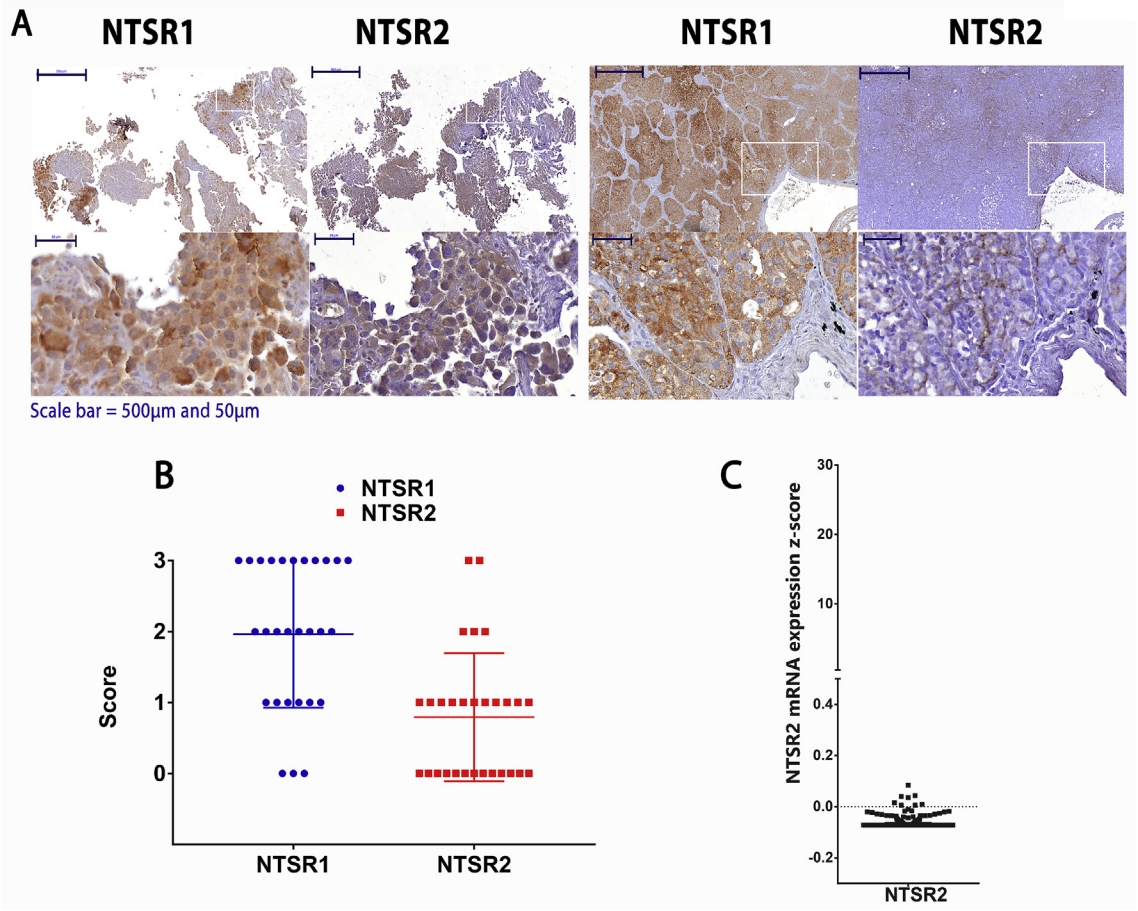

Fig. 2. NTSR2 expression in NSCLC. **A)** Immunohistochemistry of NTSR1 and NTSR2 in metastatic stages of non-squamous NSCLC patient biopsies. Two examples of positive staining is shown at X50 and X400 magnification. **(B)** Score distribution for NTSR1 and NTSR2. **(C)** NTRS2 mRNA distribution (Z-score) of 305 tumor samples from stage IB to IV of lung adenocarcinoma (TCGA-LUAD).

2.3. Immunohistochemistry

Immunohistochemistry was performed as previously described by Alifano et al. [28]. The slides were incubated at 4 °C overnight with primary antibody including LF-NTS mAb (1:200), anti-NTSR1 (1:100; SC-7596, Santa Cruz Biotechnology®), anti-NTSR2 (1:100; ANT-016, Alomone), Labs, anti-RIPK1 (1:400, NBP1-77077, Novus biological®), anti-RIPK3 (1:400, NBP1-77299, Novus biological®), anti-Ki67 (1:400, cell signaling®). The slides were then incubated with the kit starr trek universal HRP Detection System (Biocare medical®) or with Biotinylated anti-goat IgG (Vector laboratories, Inc) for NTSR1. The antigen-antibody complex was revealed with avidin-biotin peroxidase complex, according to the manufacturer's instructions (Trekavidin-HPR label, Biocare medical®). The staining was performed with diamino-benzidine tetrahydrochloride. All specimens were scored by pathologists (NH, JFF) as follows: 0: positive staining of < 10% of tumor cells; 1: positive staining involving > 10% and < 50% of tumor cells; 2: strong positive staining involving > 50% of tumor cells. For qualitative analysis (positive/negative) scores 0, 1 and 2 were pooled in the same group.

Detection of metastatic epithelial cells were performed with pan-cytokeratin (AE1/AE3 + 5D, 1/400, ab86734, Abcam®) antibodies for 30 min and revealed by the Novolink™ Polymer Detection Systems (Leica®). *In situ* cell death detection kit (Roche®, Germany) was used for TUNEL assay according to the manufacturer instructions. All the slides were scanned with 3DHISTECH scanner and analyzed with Pannoramic viewer. The integrated density was calculated as follows; the chosen color was selected in adobe photoshop, copied into a new image and transformed in gray scale. The integrated density was calculated using ImageJ software, after have inverted the image. This method was previously validated the score performed by a pathologist for the expression of NTSR1 in endometrial cancer [29].

2.4. Statistical analysis

Overall survival rates were estimated using the Kaplan-Meier method and a comparison of survival curves was performed using the log-rank test. Disease-free survival (DFS) time was calculated from the date of the initial treatment until disease recurrence (either local or distant), or the last follow-up examination.

2.5. Antibody

Monoclonal long fragment NTS antibody (LF-NTS mAb) was generated against a peptide conjugated with bovine thyroglobulin as a carrier protein, then selected by ELISA using the peptide conjugated with albumin (BioGenes GmbH). To optimize the selection of neutralizing antibodies we located the antigen peptide just upstream of the N-terminal side of Neuromedin N.

2.6. Tumor xenografts

Athymic 4-week-old male NMRI-Foxn1$^{nu/nu}$ mice (Janvier™), 5-week-old female NU (Ico)-Foxn1^{nu} mice, and 4-week-old male C57BL/6j (Janvier™) were used for human lung cancer cells xenografts, patient-derived xenografts (PDX) and the mouse lung carcinoma cell line, respectively. The ellipsoid formula was used to calculate the tumor

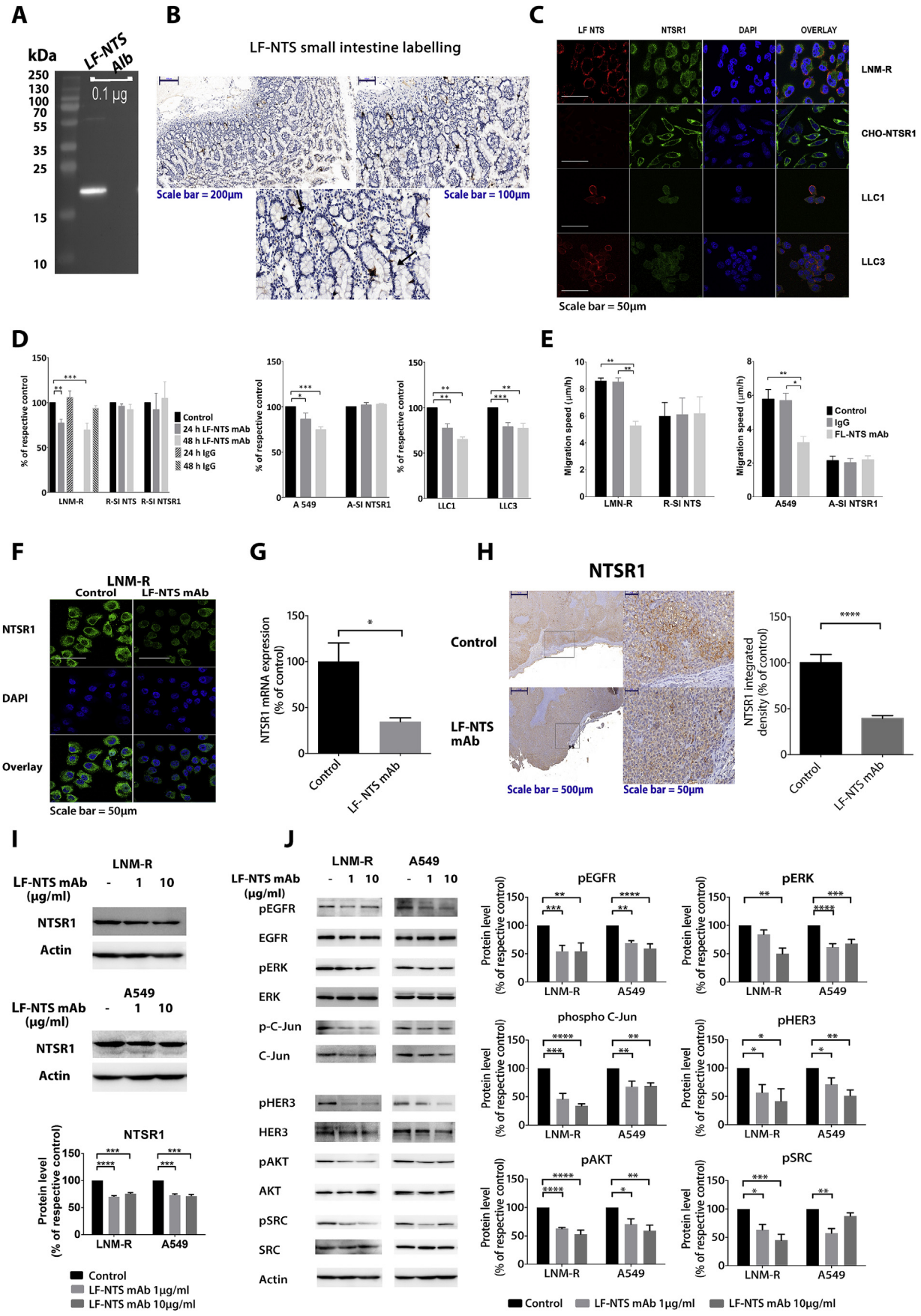

(caption on next page)

Fig. 3. NTS antibody characterization. (**A**) SDS PAGE loaded with 0.1 µg of human LF-NTS or albumin and revealed with LF-NTS mAb (2.5 µg/ml). (**B**) Immunohistochemistry of LF-NTS, example of positive staining in human intestine, at the X100, X200 magnification, below computerized magnification of a specific area. Arrows point to the labelled neuroendocrine cells. **(C)** Immunocytochemistry of LF-NTS and NTSR1 on LNM-R, CHO-NTSR1, LLC1 and LLC3 cells. Cells were stained with LF-NTS mAb (red), NTSR1 antibody (green), and DAPI (blue). **(D)** Effect of LF-NTS mAb on cell viability. LNM-R, R-SI NTSR1, R-SI NTS, A549, A-SI NTSR1, LLC1 and LLC3 were treated with 1 µg/ml of LF-NTS mAb for 24 and 48 h. This represents the mean ± SEM of at least 3 independent experiments. **(E)** Speed of migration of LNM-R and A549 cells treated or not with 10 µg/ml of LF-NTS mAb or IgG1 isotype control, on type 1 collagen. Results represent the mean ± SEM of three independent experiments. In two-way ANOVA, *p < 0.05, **p < 0.01, ***p < 0.001. **(F)** NTSR1 immunocytochemistry of LNM-R cells treated or not for 48 h with 1 µg/ml of LF-NTS mAb. Shown is the central slide from confocal microscopy, green NTSR1 and, blue DAPI. (**G**) NTSR1 mRNA level evaluated by q-PCR on LNM-R cells treated or not for 24 h with 1 µg/ml of LF-NTS mAb. In *t*-test, *p < 0.05. **(H)** (left) Example of NTSR1 and immuno-histological labelling of experimental LNM-R tumors from animals treated with PBS or LF-NTS mAb as described Fig. 4A, at 50X and 400X magnification. (right), Integrated density calculated on area of LNM-R tumor exhibiting a strong NTSR1 labelling (R 77, B 12, G12) n = 7. In *t*-test, ****p < 0.0001. **(I)** Western blot analysis of NTSR1 from LNM-R and A549 cell lysates treated or not with LF-NTS mAb for 48 h. Histograms representing intensity-based quantification of Western blot, representing the mean ± SEM of 3 independent experiments. In one-way ANOVA, ***p < 0.001. **(j)** Western blot analysis of phosphorylated form and total protein for EGFR, ERK, C-Jun, HER3, AKT, and Src, from LNM-R and A549 cell lysates, treated or not with LF-NTS mAb for 48 h (left) An example of a representative western blot. (right) Histograms representing intensity-based quantification of Western blot, representing the mean ± SEM of at least 3 independent experiments. In one-way ANOVA, *p < 0.05, **p < 0.01, ***p < 0.001, ****p < 0.0001. (For interpretation of the references to color in this figure legend, the reader is referred to the Web version of this article.)

volumes from cancer cell lines whereas the (L x W^2)/2 formula was used for PDX. When tumors reached 80–100 mm^3, groups of 7–10 mice were randomized. All the procedures were in accordance with the "Guide of the Care and Use of Laboratory Animals". Institutional Review Board approval was obtained by « Le Comité d'Ethique en l'Expérimentation Animale Charles Darwin #B751201».

2.7. PDX

This experiment was outsourced at the Curie Institute (Dr Decaudin). Lung adenocarcinomas LCF-9 PDX, scored PT2 N0, and LCF-26 PDX, scored PT2 N1, were grafted at the junction between the neck and the back in NU (Ico)-Foxn1nu female mice at 5 weeks old.

2.8. Cell culture

The lung cancer cell lines, LNM-R [25], A549 (CCL-185™), LLC1 (CRL-1642™), were grown in DMEM (Gibco®). The LLC1 cell line was sub-cloned by limiting dilution. After few days of culture, clones containing exclusively fusiform cells at high density were named LLC3. All cells were purchased at ATCC®, supplemented with 10% fetal bovine serum (FBS) (Gibco®) and 2 mM glutamine and grown at 37 °C, in a humidified atmosphere of 5% CO_2.

2.9. Cell viability assay and in vitro migration assay

15 000 cells/well were seeded in 48-well dishes. Medium was replaced by 1% FBS medium in presence or absence of LF-NTS mAb after 15 h of incubation. Cellular growth was evaluated by Z2 cell and particle counter (Beckman coulter®) after 24 h and 48 h of treatment [25]. The migration assays were carried out using two chamber inserts (ibidi®), in dishes coated with type I collagen (400µl/well, 50 µg/ml, Sigma®) as previously described [27].

2.10. RNA extraction, RT-PCR, and quantitative RT-PCR

Total RNA was extracted with guanidinium thiocyanate-phenol-chloroform acid method modified by Souaze and colleagues [30]. Primer sequences and details are described in supplementary methods.

2.11. Immunocytochemistry

The primary antibody used were LF-NTS mAb, diluted to 1/500, goat polyclonal anti-NTSR1 antibody, C-20, Santa Cruz Biotechnology®, SC-7596, diluted to 1/100, rabbit anti-phosphoHistone H2A.X(Ser139) (1:400, #9718, Cell Signalling®, diluted to 1/400. Slides were incubated for 2 h at room temperature with their respective fluorescent secondary antibody. Nuclei were counterstained with DAPI 1:50000 then mounted using ProLong® Gold Antifade Reagent (Life technologies®).

2.12. SDS-PAGE and Western blotting analysis

Western blots were processed as previously described [25] (see details in supplementary methods).

2.13. Measurement of platinum uptake in whole cell and accumulation in DNA

Platinum accumulation in whole cell and in DNA was determined by Inductively Coupled Plasma Mass Spectrometry (ICP-MS) analysis as described by Liu et al. and detailed in supplementary methods [31].

2.14. Plasma biochemical analysis

Total cholesterol, triglycerides, HDL-cholesterol, glucose, total protein and albumin were determined using a benchtop biochemistry analyzer according to the manufacturers' protocol (Randox Laboratories Ltd, Roissy en France, France).

2.15. Fecal lipid content

Feces were collected from mice housed individually over a 48-h period. Feces were dried at 60 °C for 24 h, powderized in water (5 mL for 300 mg) and then incubated with 5 mL of chloroform-methanol (2:1). Details for fecal lipid extraction are described in supplementary methods.

3. Results

3.1. NTSR1 over-expression is correlated with worse sensitivity to platinum-based chemotherapy in NSCLC patients

LF-NTS and NTSR1 expression were analyzed by immunohistochemistry from the biopsies of 28 patients with advanced stage non-squamous NSCLC. An example is shown in Fig. 1A. NTSR1 labeling was mainly restricted to the cytoplasm with clear reinforcement in certain areas. In contrast, LF-NTS labeling was mostly intracytoplasmic with a similar strong intensity throughout the sample. The scoring of NTS and NTSR1 revealed the following distribution: 11% NTSR1/0; 21% NTSR1/1, 29% NTSR1/2, and 39% NTSR1/3, while NTS labeling was scored 2 and 3 in 42% and 58% of the specimens, respectively. Concomitant expression of NTSR1 and NTS within the tumor suggests a high and sustained autocrine neurotensinergic regulation. Using the first post-chemotherapy radio-clinical evaluation (RECIST criteria), a significant more progressive disease was detected in the subset of patients exhibiting the highest NTSR1 score. These results

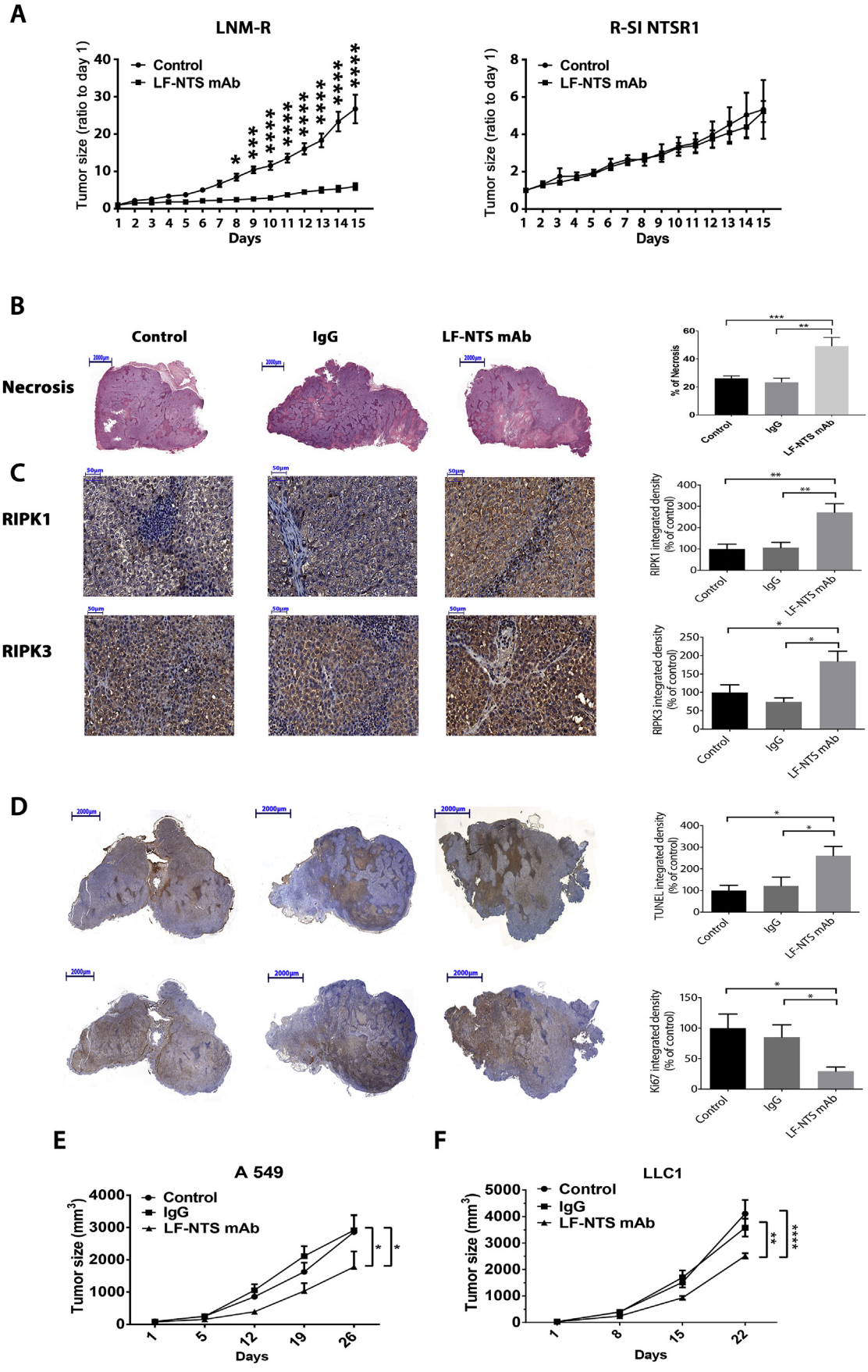

(caption on next page)

Fig. 4. LF-NTS mAb reduces the tumor growth. (A) Tumor growth curves of LNM-R and R-SI NTSR1 tumors. R-SI NTSR1 cells (10^6) were injected subcutaneously into the right flank of male NMRI-Foxn1$^{nu/nu}$ mice, LNM-R (10^6) were injected in the other flank. A week later, two groups were formed, one group was treated every other day with LF-NTS mAb (15 mg/kg) (i.p.) (n = 7). The second group was treated under the same condition with PBS (n = 9). **(B to D)** Analysis of LNM-R tumors from mice treated with PBS, LF-NTS mAb or IgG1 isotype control (15 mg/kg every 2 days for 15 days). Slides were scanned with 3DHISTECH scanner and analyzed with Pannoramic viewer at the X1 and X40 magnification. Staining estimation was made on the entire sample using the integrated density calculation. In one-way ANOVA, *p < 0.05, **p < 0.01, ***p < 0.001. **(B)** (left) Example of Hematoxylin-Eosin staining at X10 magnification. (Right) Quantification of the necrotic surface (R195, G110, B150) as compared to the entire surface of the sample. **(C)** (left) Example of RIPK1, RIPK3 labelling at X400 magnification. (Right) Graph of integrated density calculated on the strong labelling for RIPK1 (R132, G110, B108) and for RIPK3 (R150, G110, B105). Result is expressed as percentage of control. **(D)** (left) Example of TUNEL and Ki67 staining at X10 magnification. (Right) Graph of integrated density calculated on the labelling corresponding to the TUNEL assay after the necrosis zones were erased (R128, G99, B94), and the labelling corresponding to Ki67 (R130, G100, B95). Result is expressed as percentage of control. *(E) A549 cells ($5X10^6$) were injected subcutaneously into a male NMRI-*Foxn1$^{nu/nu}$ *mice (n = 6). When tumors reached* 80 mm^3*, mice were treated once a week (i.v.) with PBS, or with* 5 mg/kg of LF-NTS mAb, or mouse IgG1 isotype control (BioXcell®). **(F)** LLC1 cells (5×10^5) were injected subcutaneously into a male C57BL/6JRj (n = 8). When tumors reached 30 mm^3, mice were treated once a week (i.v.) with PBS, or with 5 mg/kg of LF-NTS mAb, or mouse IgG1 isotype control (BioXcell®). For (E) and (F) Statistical analysis: In two-way ANOVA statistical analysis, *p < 0.05, **p < 0.01, ****p < 0.0001.

suggested a reverse correlation between NTSR1 expression in tumor tissue and response to platinum salt treatment (score NTSR1 0 to 2 versus 3, p = 0.041) (Fig. 1B).

We confirmed the correlation between NTSR1 mRNA expression and the chemotherapy response in resected NSCLC patients at stage IB to IIIA using the randomized controlled trial JBR.10, which compared 71 patients treated with vinorelbine/cisplatin (ACT) to 62 patients treated by surgery alone (OBS) [32]. In the ACT group, NTSR1 over-expression was correlated with a worse survival. The overall 5-year survival was 46.15% [19.16–69.65%], 80.19% (67.06–88.51%] and 53.93% [40.56–65.54%] for patients over-expressing NTSR1 ($\geq 80^{th}$ p), without over expression ($< 80^{th}$ p), and observational group, respectively. Interestingly, in the ACT group, log rank analysis was significantly different for NTSR1 ($\geq 80^{th}$ p) *vs* NTSR1 ($< 80^{th}$ p, p = 0.0360) (Fig. 1C). A significant difference was also detected between NTSR1 ($< 80^{th}$ p *vs* OBS group p = 0.0264), but no significant difference was seen between NTSR1 ($\geq 80^{th}$ p) *vs* the OBS group (p = 0.4151), suggesting that high expression of NTSR1 in treated group results in similar outcome as those in the absence of treatment.

Moreover, in a second study of 305 lung adenocarcinomas (stage IB to IV) from the TCGA-LUAD database [33,34], the NTSR1 mRNA (z-score) distribution was heterogeneous with 20% of the specimens overexpressing NTSR1 (Fig. 1D). The degree of NTSR1 expression significantly influenced the outcome (p = 0.0082), as patients with NTSR1 expression $\geq 80^{th}$ p showed 5-year DFS of 22.85% [10.02–38.78%] whereas those with $< 80^{th}$ p showed 5-year DFS of 31.65% [23.49–41.40%]. The median of DFS was 22.6 months for patients with overexpressed NTSR1 and 31.0 months for the others (Fig. 1E). In this database, 148 (48.5%) patients progressed or recurred after initial treatment and 157 (51.5%) were disease free. Higher NTSR1 mRNA expression was significantly associated with patients in disease progression or recurrence (p = 0.0329) (Fig. 1F). We concluded that NTSR1 is a protein marker associated with tumor aggressiveness and drug resistance.

NTSR2 was similarly studied. Immunohistochemistry performed on the 28 biopsies patients with advanced stage non-squamous NSCLC showed weak or no labelling. When expressed, NTSR2 labeling was mainly within the cytoplasm, showing a distribution different from that observed with NTSR1; examples are shown in Fig. 2A. The scoring of NTSR2 revealed the following distribution: 45% NTSR2/0, 38% NTSR2/1, 10% NTSR2/2, and 7% NTSR2/3. The scoring distribution is diametrically opposite of that from the NTSR1 scoring (Fig. 2B). The distribution of NTSR2 mRNA extracted from the TCGA-LUAD database confirmed the weak and homogenous expression as compared to NTSR1 (Fig. 2C). Analysis of patients based on the expression of NTSR2 in the JBR.10, and the TCGA-LUAD databases, showed no correlation with the OS as observed for NTSR1 (data not show).

3.2. Characterization of long fragment-neurotensin antibody

We developed an antibody against the human long-fragment neurotensin, with the intent to disrupt the chronic activation of NTSR1. The monoclonal antibody (mAb) against LF-NTS was generated from a peptide, conjugated with bovine thyroglobulin as a carrier protein, and then selected by Elisa using the peptide conjugated with albumin (BioGenes GmbH). Neutralizing properties of the clones were screened by their ability to counteract the growth inhibition of CHO over-expressing NTSR1 cells induced by conditioned media from the LNM-R cells, a lung cancer cell line over-expressing NTS and NTSR1 [28], (data not shown see the procedure in Ref. [35]). The specificity of the purified antibody from selected clones was tested by western blots using a purified human long-fragment synthesized in *E. coli* (Antibodies-on line inc). A strong band was revealed by LF-NTS mAb on a western blot loaded with histidine tagged LF-NTS, whereas no band was detected on the lane loaded with albumin (Fig. 3A).

In the periphery, NTS is mainly synthesized and released by the enteroendocrine cells (N cells) of the intestine, this area represents the site referent to localize NTS. We confirmed the antibody specificity by immunohistochemistry on human small intestine (Ileum). A strong labelling of neuroendocrine cells dispersed within the epithelial cell of the intestinal mucosa was detected (Fig. 3B). Immunocytochemistry performed on LNM-R, showed a strong labelling of LF-NTS at the periphery of the cells. In contrast, NTSR1 labeling was dispersed in the cytoplasm, corresponding to the internalized form of the receptor [22,23]. As a negative control for neurotensin, no red staining corresponding to LF-NTS was seen in CHO cells overexpressing NTSR1, while exhibiting a strong NTSR1 labelling at the membrane (Fig. 3C). LF-NTS mAb also cross-reacted with mouse LF-NTS. Immunocytochemistry performed on LLC1 cells, a mouse lung carcinoma, and its subclone LLC3 (both expressing NTS and NTSR1) showed LF-NTS labelling at the surface of the cells (Fig. 3C).

We validated the neutralizing effect of LF-NTS mAb on cell growth and migration. LF-NTS mAb inhibited cellular growth on several models (LNM-R, A549, LLC1 and LLC3) by 20–30% (Fig. 3D). We also showed that the LF-NTS mAb decreased the migration speed of the LNM-R and A549 cells when cultured on collagen type I (Fig. 3E). No alteration in the proliferation or migration speed was detected when mouse total IgG was used, or when NTS or NTSR1 expression was silenced (R-SI NTS and R-SI NTSR1 are LNM-R cells silenced for NTS and NTSR1 respectively, A-SI NTSR1 are A 549 cells silenced for NTSR1) [28].

Our previous work demonstrated that the chronic and sustained activation of cancerous cells by NTS, increased NTSR1 expression. In turn, this effect generated epidermal growth factor receptor autocrine loops, induced from the release and activation of their respective ligands [22–26]. The purpose of this work was to develop a NTS proform antibody to counteract NTSR1 expression and activation, with consequently a deactivation of the oncogenic endpoint targets associated with sustained activation of NTSR1. To address these questions, we first studied NTSR1 expression under LF-NTS mAb exposure. The labelling of NTSR1 declined when LNM-R cells cultured with 0% FBS are treated with LF-NTS mAb for 48 h (Fig. 3F). Similar observations were made when cells are cultures in 5% FBS (data not shown). NTSR1 mRNA

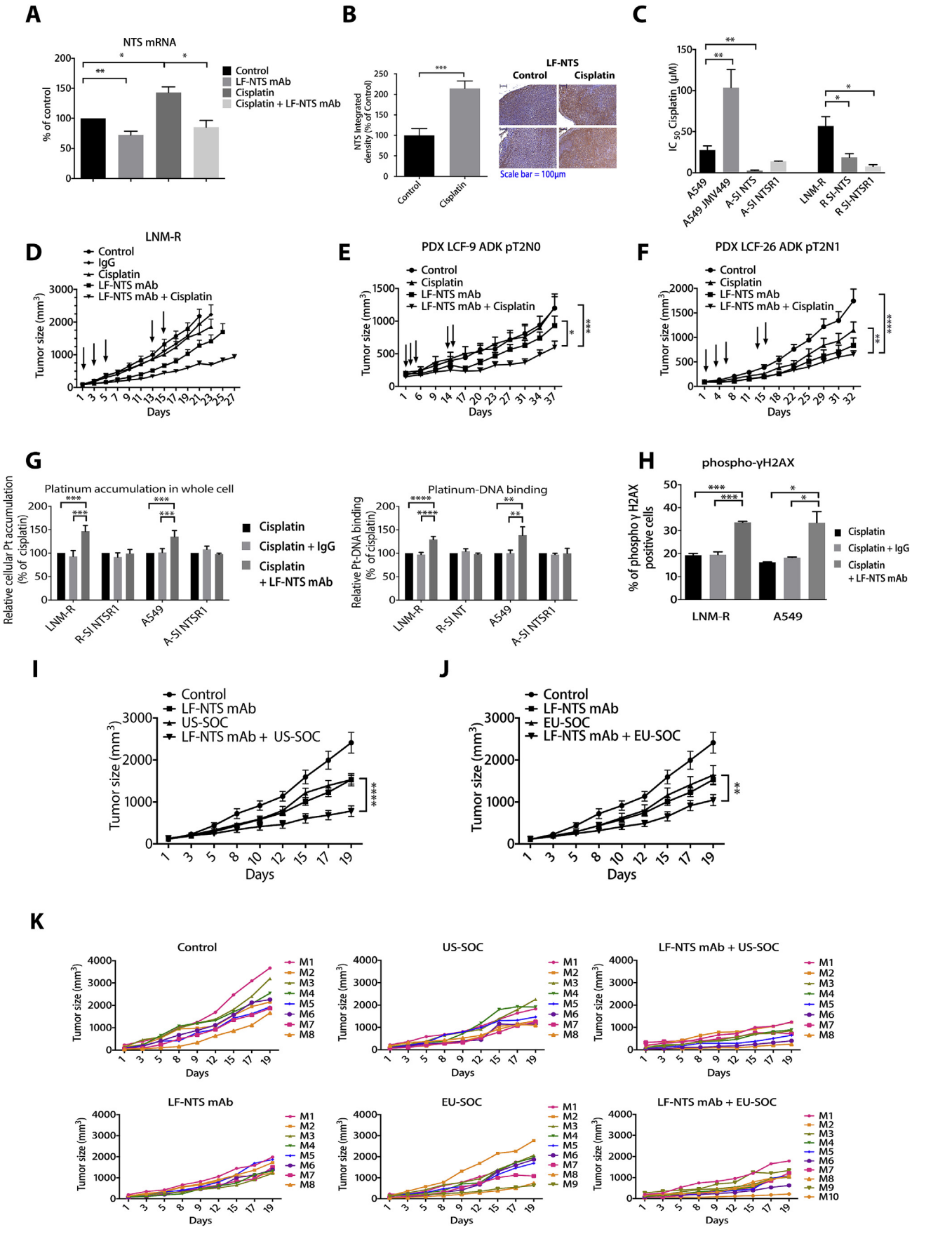

(caption on next page)

Fig. 5. LF-NTS mAb improves the response to platinum-salt based treatment. (**A**) NTSR1 mRNA quantification by qRT-PCR in LNM-R cells treated with cisplatin, LF-NTS mAb, or the combination for 24 h. Results represent the mean ± SEM of 3–4 independent experiments. In one-way ANOVA, *p < 0.05, **p < 0.01. (**B**) (left) Integrated density calculated on area of the tumor exhibiting a strong LF-NTS labelling (R124, B95, G105). n = 9, In *t*-test, ***p < 0.001. (right) Example of NTS and immuno-histological labelling of LNM-R experimental tumors from animals treated with PBS, or cisplatin (see detail in Fig. 5D), at 200X magnification. (**C**) IC_{50} calculation of A549, A-SI NTS, A-SI NTSR1, LNM-R, R-SI NTSR1 and R-SI NTS cells viability inhibition by cisplatin. Viability test was performed after 72 h of treatment. IC_{50} calculation of A549 cells in the presence or not of 10^{-8} M NTS agonist, JMV 449. Results represent the mean ± SEM of 3–4 independent experiments. In *t*-test, *p < 0.05, **p < 0.01. (**D**) LNM-R tumor size with time of mice bearing double tumors LNM-R and R-SI NTSR1 (10^6 cells). Groups of 8 mice were treated (i.p.) as followed; PBS, mouse IgG1 isotype control, LF-NTS mAb, cisplatin, or cisplatin + LF-NTS mAb. The doses were 1 mg/kg of cisplatin (indicated by the arrows) on day 1, 3, 5, 13, 15, and 15 mg/kg of LF-NTS mAb or IgG injected every other day, or both. In two-way ANOVA, at days 23, LF-NTS mAb *vs.* Cisplatin p = 0.0206; LF-NTS mAb *vs.* LF-NTS mAb + cisplatin p = 0.0001; Cisplatin *vs.* LF-NTS mAb + cisplatin p < 0.0001. R-SI NTSR1 tumor size with time is shown in Fig. S3. (**E and F**) This experiment was outsourced at institute Curie (Dr Decaudin). 2 mm^3 of tumor from two patients scored pT2N0 (E) and pT2N1 (F) were grafted at the junction between the neck and the back of NU (Ico)-Foxn1^{nu} female mice. When tumors reached 100 mm^3, mice were treated three times per week (i.p.) with PBS, or LF-NTS mAb (15 mg/kg), or 1 mg/kg cisplatin (indicated by the arrows) at day 1, 3, 5, 13, and 15 or both. In two-way ANOVA, *p < 0.05, **p < 0.01, ***p < 0.001, ****p < 0.0001. (**G**) LF-NTS mAb increases platinum accumulation in whole-cell extracts and in purified DNA of LNM-R and A549 cells. The cells were treated with 4 µmol/L cisplatin alone, or with 1 µg/ml IgG1 isotype control, or 1 µg/ml LF-NTS mAb for 48 h. The results were normalized by the total protein or DNA content. The result represents the mean ± SEM of at least three independent experiments. (**H**) Immunocytochemistry of phospho-γH2AX, on LNM-R and A549 cells pretreated or not with 1 µg/mL IgG1 isotype control or 1 µg/mL LF-NTS mAb for 18 h prior to a treatment with 32 µM cisplatin for 6 h. Number of positive cells calculated on 10 fields of 3 independents experiments, expressed as % of positive cells. For (G) and (H) In a one-way ANOVA, *p < 0.05, **p < 0.01, ***p < 0.001, ****p < 0.0001. **(I)** Xenograft of 1 million LNM-R cells treated with PBS or LF-NTS mAb (5 mg/kg once a week), or US-SOC (4 mg/kg carboplatin at day 1, 3, 5, and 30 mg/kg Pemetrexed (Alimta™) at day 1, 3, 5, and 8), or both. (**J**) Xenograft of 1 million LNM-R cells treated with PBS or FL-NTS mAb (5 mg/kg once a week), or EU-SOC (1 mg/kg cisplatin at day 1, 3, 5, and 10 mg/kg Paclitaxel (Taxol ™) at day 1, 3, 5, and 8), or both. For (I) and (J) In a two-way ANOVA, **p < 0.01, ****, p < 0.0001. (**K**) Individual follow up of LNM-R tumor size treated with PBS or LF-NTS mAb (5 mg/kg once a week), or US-SOC (4 mg/kg carboplatin at day 1, 3, 5, and 30 mg/kg Pemetrexed (Alimta™) at day 1, 3, 5, and 8), or both, or EU-SOC (1 mg/kg cisplatin at day 1, 3, 5, and 10 mg/kg Paclitaxel (Taxol ™) at day 1, 3, 5, and 8), or both.

levels also decreased under the same conditions (Fig. 3G). NTSR1 immunohistochemistry performed on LNM-R experimental tumors showed a heterogeneous labelling toward all tumors, with large zones where NTSR1 labeling was exceedingly reinforced. In animals treated with LF-NTS mAb, these reinforced zones mostly disappeared. We compared the expression of NTSR1, based on these high staining zones, between animals treated with PBS or with LF-NTS mAb by calculating the integrated density for the NTSR1 staining. The results showed a 60% decrease in NTSR1 expression (Fig. 3H).

The NTS/NTSR1 signaling is known to be upstream of several major oncogenic pathways involved in the proliferation, invasion, and metastasis, such as MAPK and PI3K/AKT pathways, and Src kinase [36,37]. We used two human lung adenocarcinoma cell lines, LNM-R and A549, to monitor the inhibition of phosphorylated kinases following LF-NTS mAb treatment, and associated with the down regulation of NTSR1 expression (Fig. 3I and J). LF-NTS mAb markedly reduced phosphorylation of several proteins engaged in the cancer progression, including EGFR, HER3, Src, Akt and ERK. No signification change was observed in the total amount of these proteins (Fig. 3J).

3.3. LF-NTS mAb decreases tumor growth

LF-NTS antibody was tested on tumor growth using a double tumor animal model grafted with LNM-R cells and R-SI NTSR1. The LNM-R cell line was chosen because it generates tumors with high growth speed and rapid lymph node metastasis [28], whereas R-SI NTS or R-SI NTSR1 display reduced tumor growth rates and metastasis processes [28]. As shown in Fig. 4A LNM-R tumor size was reduced by 65% in the LF-NTS mAb treated animals, whereas the tumor growth rate remained similar for R-SI NTSR1. At the end of the experiment, the tumors labeled with hematoxylin and eosin were analyzed. The integrated density calculated on the pale pink color, corresponding to the necrosis area showed two folds more necrosis in animals treated with LF-NTS mAb as compared to control animals (Fig. 4B). The same methodological approach showed a sharp increase in the expression of the major actors of the necroptosis pathway, RIPK1 and RIPK3, under LF-NTS mAb treatment (Fig. 4C). Moreover, twice more apoptosis (TUNEL assay), and thrice less proliferation (Ki67 assay) were observed when animals were treated with LF-NTS mAb, as compared to controls (Fig. 4D). Completing this experiment, the dose response and the schedule of the LF-NTS antibody were optimized on LNM-R cells, to 5 mg/kg injected intraperitoneal once a week (Fig. S1).

We also confirmed the effect of LF-NTS antibody on tumor growth generated by the human adenocarcinoma cell line, A549, and the mouse carcinoma cell line, LLC1 [28]. The tumor size was reduced by 40% when mice were treated intravenously with LF-NTS mAb as compared to controls (Fig. 4E and F). In summary, we observed reduced tumor aggressiveness due to LF-NTS mAb treatment.

3.4. LF-NTS mAb restores cisplatin response

It was previously shown on normal rats that platinum salts treatment significantly increased plasma neurotensin level, in association with peripheral neurotoxicity [38]. Based on this observation, we evaluated the effect of cisplatin on NTS expression, and accordingly on cisplatin resistance. A 50% increase of NTS mRNA was observed when LNM-R cells were exposed to cisplatin for 24 h. This increase was counteracted by LF-NTS mAb (Fig. 5A). Likewise, in LNM-R tumors, LF-NTS expression was higher by 50% in animals treated with cisplatin as compared to control animals (Fig. 5B). Additionally, as indicated in Fig. 5C, an alteration of cisplatin sensitivity of the lung cancer cells with NTS or NTSR1 expression was detected. A549 cells exhibited a sensitivity to cisplatin in dose-dependent manner with an IC_{50} of 27.3 ± 5.3 µM. Addition of NTS agonist (JMV449) on A549 cells increased the IC_{50} by four times to 103.7 ± 22 µM, whereas cells silenced for NTS and NTSR1 (A-SI NTS and A-SI NTSR1) showed a higher sensitivity to cisplatin (Fig. 5C). Similar observations were made with LNM-R cells (Fig. 5C).

In subsequent experiments, we tested the antibody in combination with cisplatin on tumor growth. In order to simulate clinical context, we purposely chose to treat the mice with a sub-toxic dose of cisplatin. The LD_{50} for cisplatin-injected i.p. is 12 mg/kg. Therefore, mice bearing double tumors from LNM-R and R-SI NTSR1 cells were treated 5 times with 1 mg/kg cisplatin (see Fig. 5 legend). Tumors expressing NTS/NTSR1 from LNM-R did not respond to cisplatin, whereas tumors silenced for NTSR1 were responsive (Fig. 5D and S2). The LNM-R tumors became responsive to the treatment when mice were treated with a combination LF-NTS mAb and cisplatin. The tumor size was reduced by 60% as compared to cisplatin alone treated mice (Fig. 5D). The R-SI NTSR1 tumors were responsive to cisplatin and the combined treatment did not improve the tumor growth rate (Fig. S2). Similar experiments were performed on two lung adenocarcinoma PDX models expressing NTSR1 and LF-NTS. PDX LCF-9 did not respond to the cisplatin treatment, as expected since the patient was not a responder. When the PDX

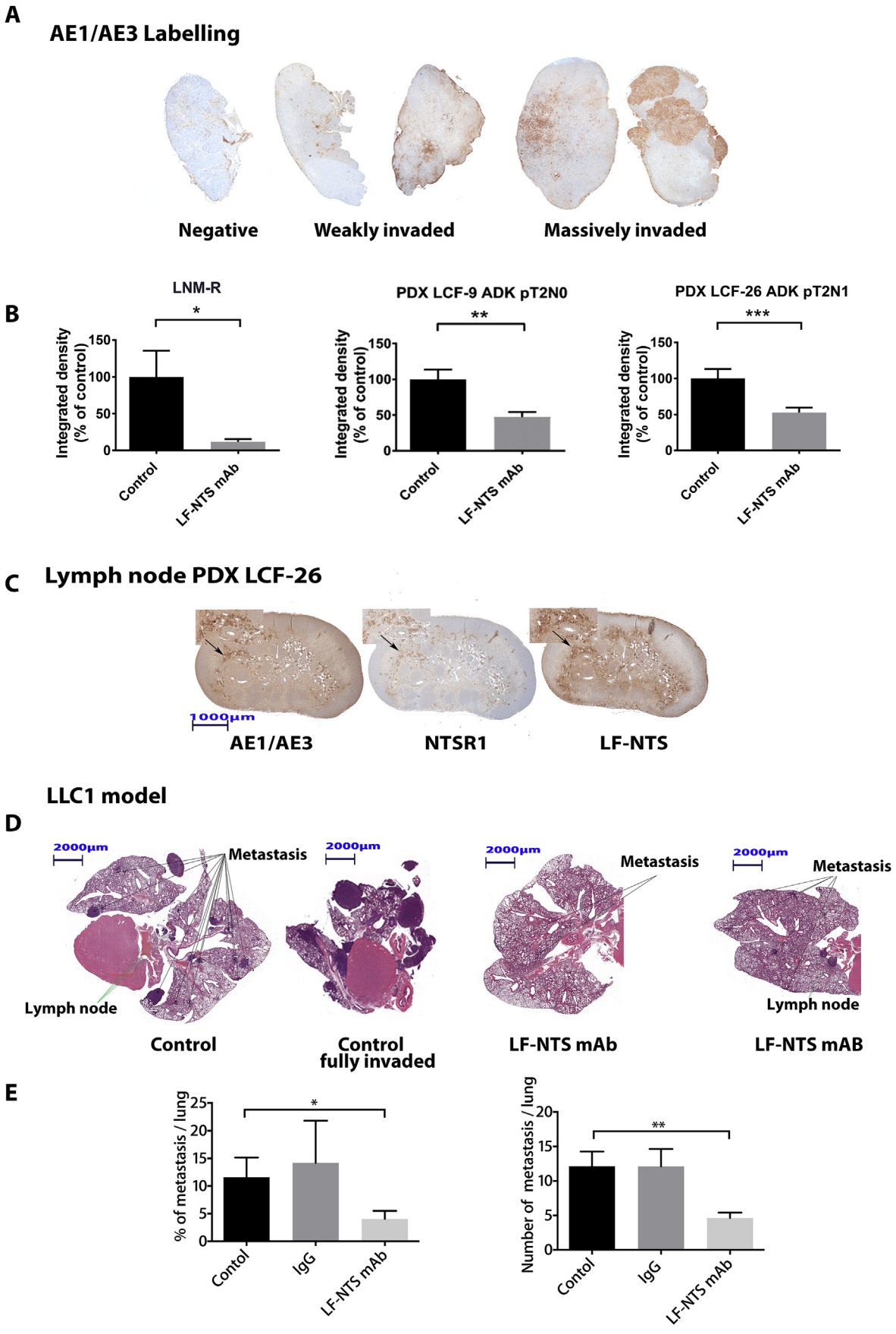

(caption on next page)

Fig. 6. LF-NTS mAb reduces metastatic process. **(A)** Typical example of lymph node labelled with AE1/AE3. **(B)** Lymph node were labelled with a cocktail of these two antibodies AE1/AE3, that recognizes the acidic and basic (Type I and II) subfamilies of cytokeratins detecting most human epithelia. Images were acquired with a Nikon Diaphot microscope at the magnification X40; the entire lymph node was reconstituted with adobe Photoshop photomerge. Cells labelling was quantified by evaluating the integrated density. Calculation was performed on ipsilateral axillary lymph node of mice bearing LNM-R (n = 7 to 9) (R213, B129, G98), and on dorsal and axillary lymph node of mice bearing PDX LCF-9 and LCF-26 (R 139, B 59, G46) (n = 16 and 20), respectively. In *t*-test, *p < 0.05, **p < 0.01, ***p < 0.001. **(C)** Example of adjacent slide of lymph node from mice bearing PDX LCF-26, labelled with AE1/AE3, NTSR1 or LF-NTS, at 20X magnification. **(D)** C57BL/6j mice were grafted with 0.5 million of a mouse lung carcinoma cell line, LLC1, at day 22, mice were sacrificed and lung metastasis were analyzed by Hematoxylin-Eosin staining at 10X magnification. **(E)** Metastases were quantified according to the percentage of invaded surface per lung and the number of metastasis per lung. Between 9 and 10 lungs were analyzed per group. In one-way ANOVA, *p < 0.05, **p < 0.01.

LCF-9 was treated with LF-NTS mAb alone, a weak response was observed. Interestingly with the combined treatment, the tumor size was reduced by 50% (Fig. 5E). The PDX LCF-26 was partially sensitive to cisplatin with a decrease of 35% of tumor size. In combination with LF-NTS mAb the effect of cisplatin on the tumor growth was doubled (Fig. 5F).

In order to evaluate the impact of LF-mAb on cells plasticity, and understand the changes of cell homeostasis induced by LF-mAb, platinum accumulation was evaluated in whole cell extracts and in nuclei. In LNM-R and A549 cells, the platinum content of the whole cell and of the nuclei (platinum bound DNA) was largely increased after 48-h exposure to the combined treatment as compared to cisplatin alone (Fig. 5G). No increase was observed in cells silenced for NTSR1 (Fig. 5G). Moreover, we analyzed the labelling of phospho-Ser139 H2AX protein (γ-H2AX), a protein known to be recruited at the site of DNA double strand breaks, in LNM-R and A549 cells after treatment with cisplatin alone or in combination with LF-NTS mAb. We detected two fold increase in the amount of positive cells when cells were pretreated with LF-NTS mAb for 18 h and then exposed to cisplatin plus LF-NTS mAb for another 6 h, as compared to cisplatin alone in both cell line (Fig. 5H and S3). These results indicated that LF-NTS mAb improved drug efficiency by enhancing the ratio of drug/target (platinum to DNA).

The first chemotherapy line of lung cancer treatment is primarily a combination of two compounds. In the USA, it is mainly the combination of carboplatin plus paclitaxel, and in Europe, it is mainly cisplatin combined with pemetrexed. Treatment of mice with a sub-toxic dose of these standards of care (SOC), showed a partial response; see US-SOC or EU-SOC (Fig. 5I and J). Co-treatment with LF-NTS mAb improved both US-SOC and EU-SOC responses. Individual responses, shown in Fig. 5K, revealed that the tumors grew at a very slow rate, or stop growing with the combination of SOC and LF-NTS mAb, especially with the US-SOC.

3.5. LF-NTS mAb reduces metastasis

We evaluated the contribution of LF-NTS mAb on metastatic processes using AE1/AE3 labelling, a cytokeratin marker for sentinel lymph node biopsies. Ipsilateral axillary lymph node of mice bearing LNM-R tumor and axillary and dorsal lymph node of mice bearing PDX were labelled with AE1/AE3. An example of the various scores of AE1/AE3 labelling is shown in Fig. 6A. Integrated density of the color corresponding to the invaded cells was calculated (Fig. 6B). The lymph nodes of mice treated with LF-NTS mAb clearly showed less metastasis (13%, 47% and 53% as compared to PBS treated mice, for LNM-R tumor, and LCF-9 or LCF-26 PDX, respectively). In addition, we observed that invasive epithelial cells in lymph node expressed NTSR1 and LF-NTS, as a representative example is shown in Fig. 6C.

We confirmed the effect of LF-NTS mAb on the metastatic process using the syngeneic LLC1 model from animals of the experiment described in Fig. 3F. The size and the number of lung metastasis were smaller in animals treated with LF-NTS mAb as compared to controls (Fig. 6D and E).

3.6. LF-NTS mAb long term treatments induced no obvious adverse events

No toxicity is expected with LF-NTS mAb long-term treatment because the epitope is localized downstream from NTS sequence. Consequently, the functions of the mature peptide NTS should not be abrogated. Long-term effects of LF-NTS mAb treatment were evaluated on C57BL/6j mice, treated once a week with 5 mg/kg for 180 days. As seen on Fig. 7A, the mice treated with NTS mAb put on weight during the treatment as compared to control mice. At day 180, antibody treated mice were 9.2% heavier than control mice. No difference in food intake was observed (data not shown). Basic blood parameters, glucose cholesterol, and triglyceride levels were not modified by the treatment. The ratio albumin to protein was significant higher in LF-NTS mAb treated mice as compared to control (Fig. 7B). No difference in food intake was observed (data not shown). The weight of feces collected during 48 h was equivalent, but the feces triglyceride and the cholesterol content was significantly higher in animals treated with LF-NTS mAb (Fig. 7C). Finally, mice treated with LF-NTS mAb were more active than controls, persisting with time (Fig. 7D). Long-term treatment with LF-NTS mAb seems to improve the biological parameters associated with quality of life and a better survival.

4. Discussion

We developed a monoclonal antibody based on a strategy to neutralize the proform of neurotensin, and thereby eliminate the oncogenic activities of NTSR1. Taking advantage of this antitumor tool, we discovered that inhibition of neurotensin enhances the toxic effects of platinum-salt based therapy. Moreover, the apparent absence of toxicity on long term treatment designates antibody-based targeting proform of neurotensin as a therapeutic promise for the improvement of chemotherapy when combined with platinum salts.

On non-transformed cells, NTS is able to induce epithelial cell proliferation, and migration, known to be major cellular effects involved in neoplasms development and progression [36]. Accordingly, upon discovery of NTS, this peptide was suspected to contribute to carcinogenesis and progression of cancer. Initiated from these observations, a large variety of studies on the contribution of NTS on cancer cells growth, migration, invasion and adherence on different type of cancers cells and tumors were designed [37]. The high affinity NTS receptor (NTSR1), a GPCR mostly coupled to Galphaq/11, activates the cascade “phospholipase C-diacylglycerol-inositol triphosphate-protein kinase C”, as well as the mobilization of intracellular calcium that regulates gene transcription, cell proliferation, migration and death [37,39]. Concurrently, NTS activates HER family (EGFR, HER2, and HER3) and creates an activating autocrine loop for these receptors in several types of cancers [25,26,40–42]. These receptors act as they all bearing driver mutations, consequently cells expressing NTS or NTSR1 are sensitive to erlotinib and lapatinib whereas the same cells depleted for NTS or NTSR1 were not responsive to these tyrosine kinase inhibitors [25–27]. Finally, NTS can also modulate the activities of the small RhoGTPases (Rac1, RhoA and Cdc42), Focal adhesion kinase, and Src, responsible for the cytoskeleton dynamics and the formation of various cytoplasmic extensions [43]. NTS activity is therefore always associated with higher tumor aggressiveness, and advanced stages.

NTSR1 was shown to be expressed in many types of cancer, whereas the original normal tissue does not express or very weakly expresses NTSR1. Activation of the wnt/β-catenin pathway and hypomethylation of the promoter were proposed as mechanisms involved in this

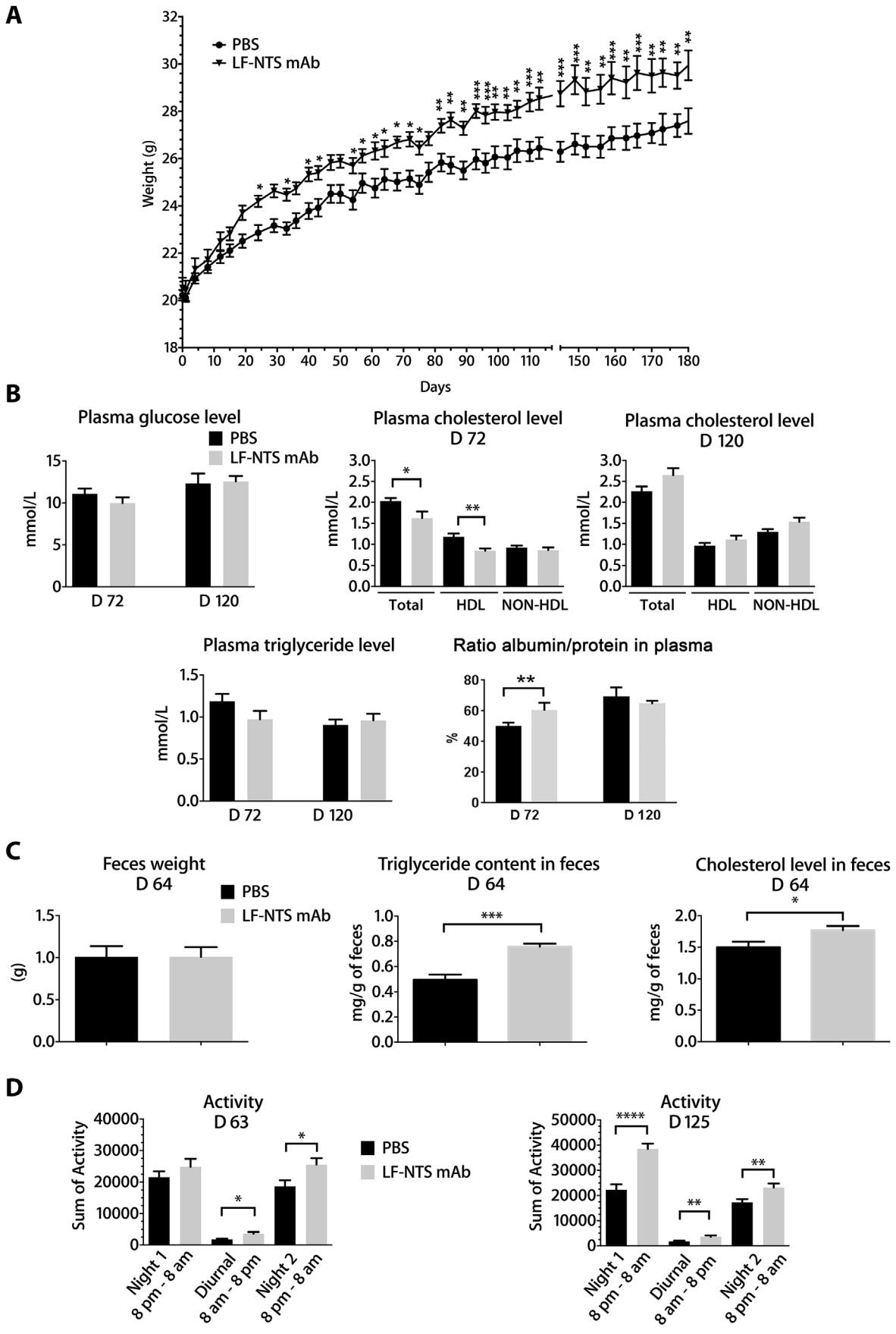

(caption on next page)

Fig. 7. LF-NTS mAb long term treatments induce no obvious adverse events. (**A**) Weight of mice treated once a week with PBS or 5 mg/kg (i.v.) LF-NTS mAb n = 10. (**B**) Glucose, cholesterol, triglyceride concentration, and ratio albumin/total protein from blood taking on fasted mice for 6 h at day 72 (n = 6), and day 120 (n = 10). (**C**) Feces weight, and triglyceride and cholesterol content in feces from 6 mice. (**D**) Mouse activity recorded from individual mouse during 48 h (ADDENFI, Les Cordeliers, Paris, France). Recording was spitted in three time period at Day 63 (n = 6), and D 120 (n = 8). From A to D In *t*-test, *p < 0.05, **p < 0.01, ***p < 0.001, ****p < 0.0001.

upregulation [30,44–46]. Furthermore, high expression of NTSR1 was associated with a pejorative prognosis and disease free survival in lung, breast and ovarian cancers, hepatocellular, endometrial, and head and neck squamous carcinomas, and gliomas [25,28,29,37,47,48]. In tumors, NTSR1 labeling was detected mainly in the cytoplasm, suggesting that NTSR1 is in an activated state. When localized in the cytoplasm, as in lung adenocarcinoma, NTSR1 expression correlates with a poor prognosis, but when it is localized at the cell surface, as in lung squamous carcinoma, NTSR1 expression has no impact on the prognosis [25]. Similar observations were made for endometrial carcinoma [29], suggesting that NTSR1 expression in tumors is not only a marker but also an actor of cancer progression. In order to decrease NTSR1 activation, we developed an antibody directed against the ligand, as NTSR1 intracellular localization rendered difficult its inhibition with an antibody, or a small molecule.

Cisplatin efficiency is limited because cells exhibit innate and acquired resistance, and it is a very toxic nonspecific compound, with its dose limitation being crucial. Many mechanisms are involved in cisplatin resistance, notably cells are able to resist induced apoptosis in response to DNA damage. Cells bypass the activation of several signal transduction pathways, including calcium signaling, death receptor signaling, and the activation of mitochondrial pathways. NTS was described as a survival factor; this was demonstrated in several cellular models from diverse cancers [37]. In particular, in breast cancer cells, NTS agonist inhibited apoptosis induced by serum deprivation, which was accompanied by the enhancement of Bcl-2 gene transcription and cellular protein content [37]. Here we show that decreasing NTSR1 activity with LF-NTS mAb not only reduced tumor cell proliferation and induced apoptosis, but also induced necrosis and the proteins involved in the necroptosis RIPK1 and RIPK3 (Fig. 4).

Limiting influx and increasing efflux are other mechanisms related with cisplatin resistance. Before reaching the DNA, cisplatin enters the cell via passive infusion or by active uptake with a number of transport proteins. Platinum can be extruded from the cells by the GS-X pumps (MRP 1-5) after chelation with glutathione or via the copper efflux system (ATP7A/B) [49]. Here, we demonstrate that blocking NTS increase the quantity of platinum in the cell and in the nucleus and, a higher amount of double strand DNA breaks. LF-NTS mAb improves cisplatin drug efficiency by improving the drug ratio to target (platinum to DNA) and by forcing cell to enter and achieve apoptosis and necrosis.

From detection at diagnosis to the fatal issue, most patients with advanced lung cancer will experience, at one point or another, platinum salt therapy alone or in combination with another compound to improve outcome. Here, we show that adding LF-NTS mAb to the standard of care (carboplatin/paclitaxel or cisplatin/pemetrexed) improves the treatment efficiency. Taking together, we propose to combine LF-NTS targeted antibody to the standard of care, and eventually maintain the treatment after several cycles of platinum salt. Preliminary studies on long-term treatment (several months) of LF-NTS antibody show that no obvious toxicity can be detected on the major blood parameters. Chow-fed animals actually gained weight under the treatment, and were more active, which may also contribute to improve the outcome. These points merit further exploration.

5. Conclusion

In summary, we have demonstrated that targeting LF-NTS enhances the response to platinum salt-based chemotherapy and reduces the tumor aggressiveness enhancing the chemotherapy-induced apoptosis and necrosis. Therapeutic strategies elaborated with LF-NTS antibody would address the most aggressive cells within a heterogeneous tumor by acting on cell plasticity, and rendering the aggressive cells manageable. As a secondary benefit, no additional toxicity should occur when used in combination with conventional treatment.

Funding

This work was supported by INSERM TRANSFERT MAT-PI-07563-A-09 (PI. Forgez), SATT IDF innov Paris, France (PI. Forgez). Dr. J. Liu was supported by China Scholarship Council, and Lund University (Sweden), Dr Z; Wu was supported by. SATT IDF innov Paris, France.

Conflicts of interest

The authors declare that they have no competing interests.

Acknowledgements

We thank Dr Neil Insdorf for his kind help in editing the manuscript. We thank Brigitte Solhonne and Fatiha Merabtene (UPMC Univ Paris 06, UMS_30 LUMIC, St Antoine Histomorphology Platform, F-75012) for their excellent assistance with the immunohistochemistry. We thank Tatiana Ledent and other staff in the animal facility of St Antoine Hospital. We also thank the microscopy platform SCM (Service Commun de Microscopie- Faculté des Sciences Fondamentales et Biomédicales-Paris)".

Appendix A. Supplementary data

Supplementary data to this article can be found online at https://doi.org/10.1016/j.canlet.2018.12.007.

References

[1] L.A. Torre, F. Bray, R.L. Siegel, J. Ferlay, J. Lortet-Tieulent, A. Jemal, Global cancer statistics, 2012, Ca - Cancer J. Clin. 65 (2015) 87–108.
[2] C. Locher, D. Debieuvre, D. Coetmeur, F. Goupil, O. Molinier, T. Collon, C. Dayen, J. Le Treut, B. Asselain, F. Martin, F. Blanchon, M. Grivaux, Major changes in lung cancer over the last ten years in France: the KBP-CPHG studies, Lung Canc. 81 (2013) 32–38.
[3] A. Sandler, R. Gray, M.C. Perry, J. Brahmer, J.H. Schiller, A. Dowlati, R. Lilenbaum, D.H. Johnson, Paclitaxel-carboplatin alone or with bevacizumab for non-small-cell lung cancer, N. Engl. J. Med. 355 (2006) 2542–2550.
[4] G.V. Scagliotti, P. Parikh, J. von Pawel, B. Biesma, J. Vansteenkiste, C. Manegold, P. Serwatowski, U. Gatzemeier, R. Digumarti, M. Zukin, J.S. Lee, A. Mellemgaard, K. Park, S. Patil, J. Rolski, T. Goksel, F. de Marinis, L. Simms, K.P. Sugarman, D. Gandara, Phase III study comparing cisplatin plus gemcitabine with cisplatin plus pemetrexed in chemotherapy-naive patients with advanced-stage non-small-cell lung cancer, J. Clin. Oncol.: Offic. J. Am. Soc. Clin. Oncol. 26 (2008) 3543–3551.
[5] I. Dagogo-Jack, A.T. Shaw, Tumour heterogeneity and resistance to cancer therapies, Nat. Rev. Clin. Oncol. 15 (2018) 81–94.
[6] K. Suda, J. Kim, I. Murakami, L. Rozeboom, M. Shimoji, S. Shimizu, C.J. Rivard, T. Mitsudomi, A.C. Tan, F.R. Hirsch, Innate genetic evolution of lung cancers and spatial heterogeneity: analysis of treatment-naive lesions, J. Thorac. Oncol.: Offic. Publ. Int. Assoc. Study Lung Canc. 13 (2018) 1496–1507.
[7] F. Barlesi, J. Mazieres, J.P. Merlio, D. Debieuvre, J. Mosser, H. Lena, L. Ouafik, B. Besse, I. Rouquette, V. Westeel, F. Escande, I. Monnet, A. Lemoine, R. Veillon, H. Blons, C. Audigier-Valette, P.P. Bringuier, R. Lamy, M. Beau-Faller, J.L. Pujol, J.C. Sabourin, F. Penault-Llorca, M.G. Denis, S. Lantuejoul, F. Morin, Q. Tran, P. Missy, A. Langlais, B. Milleron, J. Cadranel, J.C. Soria, G. Zalcman, Routine molecular profiling of patients with advanced non-small-cell lung cancer: results of a 1-year nationwide programme of the French Cooperative Thoracic Intergroup (IFCT), Lancet (London, England) 387 (2016) 1415–1426.
[8] C.K. Lee, L. Davies, Y.L. Wu, T. Mitsudomi, A. Inoue, R. Rosell, C. Zhou, K. Nakagawa, S. Thongprasert, M. Fukuoka, S. Lord, I. Marschner, Y.K. Tu, R.J. Gralla, V. Gebski, T. Mok, J.C. Yang, Gefitinib or erlotinib vs chemotherapy for EGFR mutation-positive lung cancer: individual patient data meta-analysis of

overall survival, J. Natl. Cancer Inst. 109 (2017).
[9] S. Peters, D.R. Camidge, A.T. Shaw, S. Gadgeel, J.S. Ahn, D.W. Kim, S.I. Ou, M. Perol, R. Dziadziuszko, R. Rosell, A. Zeaiter, E. Mitry, S. Golding, B. Balas, J. Noe, P.N. Morcos, T. Mok, Alectinib versus crizotinib in untreated ALK-positive non-small-cell lung cancer, N. Engl. J. Med. 377 (2017) 829–838.
[10] Z. Piotrowska, M.J. Niederst, C.A. Karlovich, H.A. Wakelee, J.W. Neal, M. Mino-Kenudson, L. Fulton, A.N. Hata, E.L. Lockerman, A. Kalsy, S. Digumarthy, A. Muzikansky, M. Raponi, A.R. Garcia, H.E. Mulvey, M.K. Parks, R.H. DiCecca, D. Dias-Santagata, A.J. Iafrate, A.T. Shaw, A.R. Allen, J.A. Engelman, L.V. Sequist, Heterogeneity underlies the emergence of EGFRT790 wild-type clones following treatment of T790M-positive cancers with a third-generation EGFR inhibitor, Cancer Discov. 5 (2015) 713–722.
[11] D.M. Pardoll, The blockade of immune checkpoints in cancer immunotherapy, Nature reviews, Cancer 12 (2012) 252–264.
[12] M. Reck, D. Rodriguez-Abreu, A.G. Robinson, R. Hui, T. Csoszi, A. Fulop, M. Gottfried, N. Peled, A. Tafreshi, S. Cuffe, M. O'Brien, S. Rao, K. Hotta, M.A. Leiby, G.M. Lubiniecki, Y. Shentu, R. Rangwala, J.R. Brahmer, Pembrolizumab versus chemotherapy for PD-L1-positive non-small-cell lung cancer, N. Engl. J. Med. 375 (2016) 1823–1833.
[13] M.A. Postow, R. Sidlow, M.D. Hellmann, Immune-related adverse events associated with immune checkpoint blockade, N. Engl. J. Med. 378 (2018) 158–168.
[14] H.A. Yu, M.E. Arcila, N. Rekhtman, C.S. Sima, M.F. Zakowski, W. Pao, M.G. Kris, V.A. Miller, M. Ladanyi, G.J. Riely, Analysis of tumor specimens at the time of acquired resistance to EGFR-TKI therapy in 155 patients with EGFR-mutant lung cancers, Clin. Canc. Res.: Offic. J. Am. Assoc. Cancer Res. 19 (2013) 2240–2247.
[15] L.V. Sequist, B.A. Waltman, D. Dias-Santagata, S. Digumarthy, A.B. Turke, P. Fidias, K. Bergethon, A.T. Shaw, S. Gettinger, A.K. Cosper, S. Akhavanfard, R.S. Heist, J. Temel, J.G. Christensen, J.C. Wain, T.J. Lynch, K. Vernovsky, E.J. Mark, M. Lanuti, A.J. Iafrate, M. Mino-Kenudson, J.A. Engelman, Genotypic and histological evolution of lung cancers acquiring resistance to EGFR inhibitors, Sci. Transl. Med. 3 (2011) 75ra26.
[16] J.F. Gainor, L. Dardaei, S. Yoda, L. Friboulet, I. Leshchiner, R. Katayama, I. Dagogo-Jack, S. Gadgeel, K. Schultz, M. Singh, E. Chin, M. Parks, D. Lee, R.H. DiCecca, E. Lockerman, T. Huynh, J. Logan, L.L. Ritterhouse, L.P. Le, A. Muniappan, S. Digumarthy, C. Channick, C. Keyes, G. Getz, D. Dias-Santagata, R.S. Heist, J. Lennerz, L.V. Sequist, C.H. Benes, A.J. Iafrate, M. Mino-Kenudson, J.A. Engelman, A.T. Shaw, Molecular mechanisms of resistance to first- and second-generation ALK inhibitors in ALK-rearranged lung cancer, Cancer Discov. 6 (2016) 1118–1133.
[17] H.E. Bhang, D.A. Ruddy, V. Krishnamurthy Radhakrishna, J.X. Caushi, R. Zhao, M.M. Hims, A.P. Singh, I. Kao, D. Rakiec, P. Shaw, M. Balak, A. Raza, E. Ackley, N. Keen, M.R. Schlabach, M. Palmer, R.J. Leary, D.Y. Chiang, W.R. Sellers, F. Michor, V.G. Cooke, J.M. Korn, F. Stegmeier, Studying clonal dynamics in response to cancer therapy using high-complexity barcoding, Nat. Med. 21 (2015) 440–448.
[18] M. Jamal-Hanjani, G.A. Wilson, N. McGranahan, N.J. Birkbak, T.B.K. Watkins, S. Veeriah, S. Shafi, D.H. Johnson, R. Mitter, R. Rosenthal, M. Salm, S. Horswell, M. Escudero, N. Matthews, A. Rowan, T. Chambers, D.A. Moore, S. Turajlic, H. Xu, S.M. Lee, M.D. Forster, T. Ahmad, C.T. Hiley, C. Abbosh, M. Falzon, E. Borg, T. Marafioti, D. Lawrence, M. Hayward, S. Kolvekar, N. Panagiotopoulos, S.M. Janes, R. Thakrar, A. Ahmed, F. Blackhall, Y. Summers, R. Shah, L. Joseph, A.M. Quinn, P.A. Crosbie, B. Naidu, G. Middleton, G. Langman, S. Trotter, M. Nicolson, H. Remmen, K. Kerr, M. Chetty, L. Gomersall, D.A. Fennell, A. Nakas, S. Rathinam, G. Anand, S. Khan, P. Russell, V. Ezhil, B. Ismail, M. Irvin-Sellers, V. Prakash, J.F. Lester, M. Kornaszewska, R. Attanoos, H. Adams, H. Davies, S. Dentro, P. Taniere, B. O'Sullivan, H.L. Lowe, J.A. Hartley, N. Iles, H. Bell, Y. Ngai, J.A. Shaw, J. Herrero, Z. Szallasi, R.F. Schwarz, A. Stewart, S.A. Quezada, J. Le Quesne, P. Van Loo, C. Dive, A. Hackshaw, C. Swanton, Tracking the evolution of non-small-cell lung cancer, N. Engl. J. Med. 376 (2017) 2109–2121.
[19] M. Russo, G. Siravegna, L.S. Blaszkowsky, G. Corti, G. Crisafulli, L.G. Ahronian, B. Mussolin, E.L. Kwak, M. Buscarino, L. Lazzari, E. Valtorta, M. Truini, N.A. Jessop, H.E. Robinson, T.S. Hong, M. Mino-Kenudson, F. Di Nicolantonio, A. Thabet, A. Sartore-Bianchi, S. Siena, A.J. Iafrate, A. Bardelli, R.B. Corcoran, Tumor heterogeneity and lesion-specific response to targeted therapy in colorectal cancer, Cancer Discov. 6 (2016) 147–153.
[20] C. Friry, S. Feliciangeli, F. Richard, P. Kitabgi, C. Rovere, Production of recombinant large proneurotensin/neuromedin N-derived peptides and characterization of their binding and biological activity, Biochem. Biophys. Res. Commun. 290 (2002) 1161–1168.
[21] O. Melander, A.S. Maisel, P. Almgren, J. Manjer, M. Belting, B. Hedblad, G. Engstrom, U. Kilger, P. Nilsson, A. Bergmann, M. Orho-Melander, Plasma proneurotensin and incidence of diabetes, cardiovascular disease, breast cancer, and mortality, Jama 308 (2012) 1469–1475.
[22] M. Toy-Miou-Leong, C.L. Cortes, A. Beaudet, W. Rostene, P. Forgez, Receptor trafficking via the perinuclear recycling compartment accompanied by cell division is necessary for permanent neurotensin cell sensitization and leads to chronic mitogen-activated protein kinase activation, J. Biol. Chem. 279 (2004) 12636–12646.
[23] M. Najimi, F. Souaze, M. Mendez, E. Hermans, T. Berbar, W. Rostene, P. Forgez, Activation of receptor gene transcription is required to maintain cell sensitization after agonist exposure. Study on neurotensin receptor, J. Biol. Chem. 273 (1998) 21634–21641.
[24] F. Souaze, W. Rostene, P. Forgez, Neurotensin agonist induces differential regulation of neurotensin receptor mRNA. Identification of distinct transcriptional and post-transcriptional mechanisms, J. Biol. Chem. 272 (1997) 10087–10094.
[25] M. Younes, Z. Wu, S. Dupouy, A.M. Lupo, N. Mourra, T. Takahashi, J.F. Flejou, J. Tredaniel, J.F. Regnard, D. Damotte, M. Alifano, P. Forgez, Neurotensin (NTS) and its receptor (NTSR1) causes EGFR, HER2 and HER3 over-expression and their autocrine/paracrine activation in lung tumors, confirming responsiveness to erlotinib, Oncotarget 5 (2014) 8252–8269.
[26] S. Dupouy, V.K. Doan, Z. Wu, N. Mourra, J. Liu, O. De Wever, F.P. Llorca, A. Cayre, A. Kouchkar, A. Gompel, P. Forgez, Activation of EGFR, HER2 and HER3 by neurotensin/neurotensin receptor 1 renders breast tumors aggressive yet highly responsive to lapatinib and metformin in mice, Oncotarget 5 (2014) 8235–8251.
[27] Z. Wu, A. Galmiche, J. Liu, N. Stadler, D. Wendum, E. Segal-Bendirdjian, V. Paradis, P. Forgez, Neurotensin regulation induces overexpression and activation of EGFR in HCC and restores response to erlotinib and sorafenib, Cancer Lett. 388 (2017) 73–84.
[28] M. Alifano, F. Souaze, S. Dupouy, S. Camilleri-Broet, M. Younes, S.M. Ahmed-Zaid, T. Takahashi, A. Cancellieri, S. Damiani, M. Boaron, P. Broet, L.D. Miller, C. Gespach, J.F. Regnard, P. Forgez, Neurotensin receptor 1 determines the outcome of non-small cell lung cancer, Clin. Canc. Res.: Offic. J. Am. Assoc. Cancer Res. 16 (2010) 4401–4410.
[29] M. Agopiantz, P. Forgez, J.M. Casse, S. Lacomme, C. Charra-Brunaud, I. Clerc-Urmes, O. Morel, C. Bonnet, J.L. Gueant, J.M. Vignaud, A. Gompel, G. Gauchotte, Expression of neurotensin receptor 1 in endometrial adenocarcinoma is correlated with histological grade and clinical outcome, Virchows Arch. 471 (2017) 521–530.
[30] F. Souaze, V. Viardot-Foucault, N. Roullet, M. Toy-Miou-Leong, A. Gompel, E. Bruyneel, E. Comperat, M.C. Faux, M. Mareel, W. Rostene, J.F. Flejou, C. Gespach, P. Forgez, Neurotensin receptor 1 gene activation by the Tcf/beta-catenin pathway is an early event in human colonic adenomas, Carcinogenesis 27 (2006) 708–716.
[31] J. Liu, M. Agopiantz, J. Poupon, Z. Wu, P.A. Just, B. Borghese, E. Segal-Bendirdjian, G. Gauchotte, A. Gompel, P. Forgez, Neurotensin receptor 1 antagonist SR48692 improves response to carboplatin by enhancing apoptosis and inhibiting drug efflux in ovarian cancer, Clin. Canc. Res.: Offic. J. Am. Assoc. Cancer Res. 23 (2017) 6516–6528.
[32] T. Winton, R. Livingston, D. Johnson, J. Rigas, M. Johnston, C. Butts, Y. Cormier, G. Goss, R. Inculet, E. Vallieres, W. Fry, D. Bethune, J. Ayoub, K. Ding, L. Seymour, B. Graham, M.S. Tsao, D. Gandara, K. Kesler, T. Demmy, F. Shepherd, Vinorelbine plus cisplatin vs. observation in resected non-small-cell lung cancer, N. Engl. J. Med. 352 (2005) 2589–2597.
[33] J. Gao, B.A. Aksoy, U. Dogrusoz, G. Dresdner, B. Gross, S.O. Sumer, Y. Sun, A. Jacobsen, R. Sinha, E. Larsson, E. Cerami, C. Sander, N. Schultz, Integrative analysis of complex cancer genomics and clinical profiles using the cBioPortal, Sci. Signal. 6 (2013) pl1.
[34] E. Cerami, J. Gao, U. Dogrusoz, B.E. Gross, S.O. Sumer, B.A. Aksoy, A. Jacobsen, C.J. Byrne, M.L. Heuer, E. Larsson, Y. Antipin, B. Reva, A.P. Goldberg, C. Sander, N. Schultz, The cBio cancer genomics portal: an open platform for exploring multidimensional cancer genomics data, Cancer Discov. 2 (2012) 401–404.
[35] W.Y. Xu-van Opstal, C. Ranger, O. Lejeune, P. Forgez, H. Boudin, J.C. Bisconte, W. Rostene, Automated image analyzing system for the quantitative study of living cells in culture, Microsc. Res. Tech. 28 (1994) 440–447.
[36] B.M. Evers, Neurotensin and growth of normal and neoplastic tissues, Peptides 27 (2006) 2424–2433.
[37] S. Dupouy, N. Mourra, V.K. Doan, A. Gompel, M. Alifano, P. Forgez, The potential use of the neurotensin high affinity receptor 1 as a biomarker for cancer progression and as a component of personalized medicine in selective cancers, Biochimie 93 (2011) 1369–1378.
[38] M.S. Al Moundhri, S. Al-Salam, A. Al Mahrouqee, S. Beegam, B.H. Ali, The effect of curcumin on oxaliplatin and cisplatin neurotoxicity in rats: some behavioral, biochemical, and histopathological studies, J. Med. Toxicol.: Offic. J. Am. Coll. Med. Toxicol. 9 (2013) 25–33.
[39] C. Cui, R. Merritt, L. Fu, Z. Pan, Targeting calcium signaling in cancer therapy, Acta Pharm. Sin. B 7 (2017) 3–17.
[40] D. Zhao, Y. Zhan, H. Zeng, H.W. Koon, M.P. Moyer, C. Pothoulakis, Neurotensin stimulates expression of early growth response gene-1 and EGF receptor through MAP kinase activation in human colonic epithelial cells, Int. J. Canc. 120 (2007) 1652–1656.
[41] S. Hassan, P.R. Dobner, R.E. Carraway, Involvement of MAP-kinase, PI3-kinase and EGF-receptor in the stimulatory effect of Neurotensin on DNA synthesis in PC3 cells, Regul. Pept. 120 (2004) 155–166.
[42] K. Kisfalvi, S. Guha, E. Rozengurt, Neurotensin and EGF induce synergistic stimulation of DNA synthesis by increasing the duration of ERK signaling in ductal pancreatic cancer cells, J. Cell. Physiol. 202 (2005) 880–890.
[43] S. Servotte, I. Camby, O. Debeir, C. Deroanne, C.A. Lambert, C.M. Lapiere, R. Kiss, B. Nusgens, C. Decaestecker, The in vitro influences of neurotensin on the motility characteristics of human U373 glioblastoma cells, Neuropathol. Appl. Neurobiol. 32 (2006) 575–584.
[44] Z. Wu, D. Martinez-Fong, J. Tredaniel, P. Forgez, Neurotensin and its high affinity receptor 1 as a potential pharmacological target in cancer therapy, Front. Endocrinol. 3 (2012) 184.
[45] Q. Wang, Y. Zhou, B.M. Evers, Neurotensin phosphorylates GSK-3alpha/beta through the activation of PKC in human colon cancer cells, Neoplasia 8 (2006) 781–787.
[46] A.C. Tan, A. Jimeno, S.H. Lin, J. Wheelhouse, F. Chan, A. Solomon, N.V. Rajeshkumar, B. Rubio-Viqueira, M. Hidalgo, Characterizing DNA methylation patterns in pancreatic cancer genome, Mol. Oncol. 3 (2009) 425–438.
[47] S. Shimizu, J. Tsukada, T. Sugimoto, N. Kikkawa, K. Sasaki, H. Chazono, T. Hanazawa, Y. Okamoto, N. Seki, Identification of a novel therapeutic target for head and neck squamous cell carcinomas: a role for the neurotensin-neurotensin receptor 1 oncogenic signaling pathway, Int. J. Canc. 123 (2008) 1816–1823.
[48] Q. Ouyang, X. Gong, H. Xiao, J. Zhou, M. Xu, Y. Dai, L. Xu, H. Feng, H. Cui, L. Yi, Neurotensin promotes the progression of malignant glioma through NTSR1 and impacts the prognosis of glioma patients, Mol. Canc. 14 (2015) 21.
[49] M.D. Hall, M. Okabe, D.W. Shen, X.J. Liang, M.M. Gottesman, The role of cellular accumulation in determining sensitivity to platinum-based chemotherapy, Annu. Rev. Pharmacol. Toxicol. 48 (2008) 495–535.